Photochemical & Photobiological Sciences

Heck reaction synthesis of anthracene and naphthalene derivatives as traps and clean chemical sources of singlet molecular oxygen in biological systems

Journal:	*Photochemical & Photobiological Sciences*
Manuscript ID	PP-ART-04-2020-000153.R2
Article Type:	Paper
Date Submitted by the Author:	10-Aug-2020
Complete List of Authors:	Oliveira, Marilene; Instituto Federal de Educação Ciência e Tecnologia Goiano - Campus Rio Verde, Agroquímica Chorociejus, Gabriel; Universidade de Sao Paulo Instituto de Quimica, Departamento de Bioquímica Angeli, José Pedro; University of Würzburg, Rudolf Virchow Center for Translational Bioimaging Muniz Vila Verde, Giuliana; Universidade Estadual de Goias, Pharmacy Aquino, Gilberto; Universidade Estadual de Goias - Campus de Ciencias Exatas e Tecnologicas Henrique Santillo, Mestrado em Ciências Moleculares Ronsein, Graziella; Universidade de São Paulo Instituto de Química, Departamento de Bioquimica Oliveira, Maurício César ; Polícia Federal, São Paulo, Setor Técnico-Científico Barbosa, Livea ; Universidade de São Paulo Instituto de Química, Departamento de Bioquímica Medeiros, Marisa Helena Gennari de; Universidade de Sao Paulo Instituto de Quimica, Departamento de Bioquimica Greer, Alex; Brooklyn College, Department of Chemistry, City University of New York; City University of New York The Graduate Center, Ph.D. Program in Chemistry Di Mascio, Paolo; Universidade de Sao Paulo Instituto de Quimica, Departamento de Bioquimica

ARTICLE

Heck reaction synthesis of anthracene and naphthalene derivatives as traps and clean chemical sources of singlet molecular oxygen in biological systems

Received 00th January 20xx,
Accepted 00th January 20xx

DOI: 10.1039/x0xx00000x

Marilene Silva Oliveira*[1,2,3], Gabriel Chorociejus[1], José Pedro F. Angeli[4], Giuliana M. V. V. Safadi[2], Gilberto L. B. Aquino[2], Graziella E. Ronsein[1], Maurício César Bof de Oliveira[5], Livea F. Barbosa[1], Marisa H.G. Medeiros[1], Alexander Greer[6,7,] and Paolo Di Mascio*[1]

Studies have previously shown that anthracene and naphthalene derivatives serve as compounds for trapping and chemically generating singlet molecular oxygen [O_2 ($^1\Delta_g$)], respectively. Simple and efficient synthetic routes to anthracene and naphthalene derivatives are needed, for improved capture and release of O_2 ($^1\Delta_g$) in cellular environments. Because of this need, we have synthesized a dihydroxypropyl amide naphthlene endoperoxide as a O_2 ($^1\Delta_g$) donor, as well as five anthracene derivatives as O_2 ($^1\Delta_g$) acceptor. The anthracene derivatives bear dihydroxypropyl amide, ester, and sulfonate ion end groups connected to 9,10-positions by way of unsaturated (vinyl) and saturated (ethyl) bridging groups. Heck reactions were found to yield these six compounds in easy-to-carry out 3-step reactions in yields of 65-80%. Preliminary results point to the potential for the anthracene compounds to serve as O_2 ($^1\Delta_g$) acceptors and would be amenable for future use in biological systems to expanding the understanding of O_2 ($^1\Delta_g$) in biochemistry.

Introduction

Singlet molecular oxygen [O_2 ($^1\Delta_g$)] is a potent reactive oxygen species that oxidizes biomolecules including DNA, protein and lipids.[1-7] It is also a key cytotoxic species in the photodynamic therapy (PDT) of tumors, and is linked to pathophysiological effects and other processes.[8-27] But there are difficulties in producing clean sources of O_2 ($^1\Delta_g$), which make studying its reactivity challenging.

The generation of O_2 ($^1\Delta_g$) is commonly carried out in the presence of light and a photosensitizer. However, its photochemical formation (known as type II sensitized oxidation) is in competition with the formation of oxygen radicals and radical ions from type I sensitized oxidation.[28-30] Thus, clean sources of O_2 ($^1\Delta_g$) are needed.

The development of naphthalene endoperoxides as clean sources of O_2($^1\Delta_g$) in organic solvents by Wasserman et al.[31,32] and in cells by Pierlot et al.,[33,34,35] Klotz et al.,[36] Martinez et al.[37,38] was an important advancement. Naphthalene endoperoxides are unstable and thermally release O_2($^1\Delta_g$).[39-42] Pierlot et al.[33] synthesized *N,N'*-di(2,3-dihydroxypropyl)-1,4-naphthalenedipropanamide (DHPN, Fig. 1), as a naphthalene acceptor of O_2($^1\Delta_g$). The total quenching rate constant (k_T) of O_2($^1\Delta_g$) with DHPN, disodium 1,4-naphthalenediproprionate (NDP) and sodium 4-methyl-1-naphthalenepropanoate (MNP) is reasonably high at 1.0×10^6, 2.8×10^6, 7.0×10^6 M^{-1} s^{-1}, respectively (Fig. 1) [33-35,40]. Moreover, k_T values increase with electron donating groups and decrease with sterically hindered groups.[33,34] Furthermore, we have shown the clean formation of ^{18}O-labeled singlet oxygen using ^{18}O-labeled naphthalene endoperoxides.[1,21-24,37,38] Once the naphthalene endoperoxides are formed, they are labile and upon mild heating,

[1] Departamento de Bioquímica, Instituto de Química, Universidade de São Paulo, CP CP26077, CEP 05508-000, São Paulo, SP, Brazil.
[2] Instituto Federal de Educação, Ciência e Tecnologia Goiano, Departamento de Agroquímica, Campus Rio Verde, Rio Verde, Goiás.
[3]Campus Anápolis de Ciências Exatas e Tecnológicas Henrique Santillo, Universidade Estadual de Goiás, 75001-970 Anápolis, GO, Brazil.
[4]Rudolf Virchow Center for Translational Bioimaging, University of Würzburg, 97080 Würzburg, Germany.
[5] Setor Técnico-Científico, Polícia Federal, CEP 05038-090, São Paulo, SP, Brazil.
[6] Department of Chemistry, Brooklyn College, City University of New York, Brooklyn, New York 11210, United States.
[7] Ph.D. Program in Chemistry, The Graduate Center of the City University of New York, 365 Fifth Avenue, New York, New York 10016, United States.
*marilenes36@gmail.com and pdmascio@iq.usp.br.

they can be used as clean sources of $O_2(^1\Delta_g)$ in biological media, which is one of the objectives of our work. Namely, we improved the synthesis of the DHPN naphthalene derivative, by employing the Heck reaction[43,44] to reduce the total number of steps.

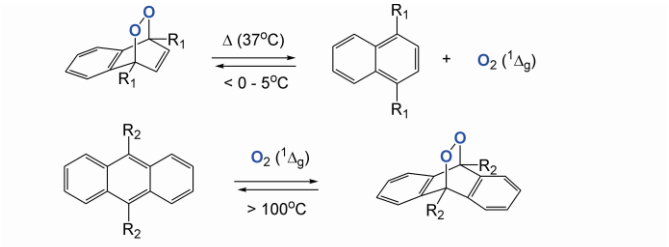

R_1 = $-CH_3$ **(DMN)**, $-(CH_2)_2COO^-$ and CH_3 **(MNP)**, $-(CH_2)_2COO^-$ **(NDP)** $-CHCHCO_2CH_2CH_3$ **(2)**, $-CH_2CH_2CO_2CH_2CH_3$ **(3)**, $-(CH_2)_2CONHCH_2CHOHCH_2OH$ **(DHPN)**

R_2 = $-CH_3$ **(DMA)**, $-C_6H_5$ **(DPA)**, $-CHCHSO_3^-$ **(8, AVS)**, $-CH_2CH_2SO_3^-$ **(AES)**, $-CHCHOSO_3^-$ **(EAS)**, $-CHCHCO_2CH_2CH_2CO_2H$ **(7)**, $-CHCHCO_2CH_2CH_3$ **(DADB, 10)**, $-CH_2CH_2CO_2CH_2CH_3$ **(11)**, $-CHCHCO_2H$ **(12)**, $-(CH_2)_2CONHCH_2CHOHCH_2OH$ **(13)**, $-(CH_2)_2CONHCH_2CHOHCH_2OH$ **(DHPA, 15)**

Figure 1. Facile thermal release of $O_2(^1\Delta_g)$ by naphthalene endoperoxide, and subsequent $O_2(^1\Delta_g)$ capture by anthracene traps to form stable anthracene endoperoxides.

A second objective of our work was to use anthracene derivatives as $O_2(^1\Delta_g)$ traps in biological media. Anthracene endoperoxides are not generally labile and retain the peroxide group, traps but do not reverse and release $O_2(^1\Delta_g)$,[45-47] and are stable under various conditions, and thus serve as indirect trapping agents for $O_2(^1\Delta_g)$. In the present work, we also employed the Heck reaction for an efficient synthetic route to anthracene derivatives. Our objective is to improve on the challenging problem of the detection of $O_2(^1\Delta_g)$ in cells. Probes such as Singlet Oxygen Sensor Green (SOSG),[48] dimethyl or diphenyl anthracene coupled with fluorescein (9-[2-(3-carboxy-9,10-diphenyl)anthryl]-6-hydroxy-3H-xanthen-3-one (DPAX), 9-[2-(3-carboxy-9,10-dimethyl)anthryl]-6-hydroxy-3H-xanthen-3-one (DMAX) are in use, but their synthesis in multisteped and cost high.[49,50] Thus, we aimed to synthesize derivatives with further substituent modifications in the 9,10-position of anthracene, which are both easy to synthesize and their corresponding endoperoxide stable for easy detection. Furthermore, we have previously shown the presence of ^{18}O-labeled singlet oxygen as confirmed by the formation of ^{18}O-labeled anthracene endoperoxides as determined by mass spectrometry.[1, 21-24,37,38] Thus, there remain needs for the facile synthesis and testing of naphthalene endoperoxides as $O_2(^1\Delta_g)$ donors and anthracenes as $O_2(^1\Delta_g)$ acceptors for biological systems. Desire for control of cell location and selectivity is of importance when evaluating the naphthalene endoperoxides as $O_2(^1\Delta_g)$ donors and anthracenes as $O_2(^1\Delta_g)$ acceptors in biological targets.[33,51-53]

In the present study, we describe the synthesis of one naphthalene (**4**) and five anthracene derivatives (**8**, **10**, **11**, **13**, and **15**). Some of the anthracene derivatives contain unsaturated C=C groups. Interestingly, the presence of a formal charge slightly diminishes the yield when using the Pd-catalyzed Heck reaction, but was successful overall in delivering yields in the range of 70-80%. We can now synthesize naphthalene endoperoxides and anthracene derivatives for the clean release and capture of O_2 ($^1\Delta_g$), respectively, in cells. The $O_2(^1\Delta_g)$ donor and acceptor compounds developed here can possibly be used in *in vivo* systems, assuming good compatibility of these compounds.

Results and discussion

Synthesis

The synthesis of DHPN is similar to Pierlot et al.[33] and Martinez et al.[37,38] and based on the photobromination of 1,4-dimethylnaphthalene, to yield 1,4-dibromomethylnaphthalene, which is subsequently purified by recrystallization in chloroform. Next malonic synthesis, hydrolysis, and decarboxylation are employed to obtain 1,4-naphthalenedipropanoic acid (NDPA), which is used to synthesize diethyl-1,4-naphthalenedipropanoate (DENDP) by acid-catalyzed esterification. The NDPA and H_2SO_4 (95%) are then refluxed in ethanol for 2h, after which a Dean-Stark trap with toluene is used. After another 4h of refluxing, DENDP, as an oil, is obtained with a yield of 87%. Finally, the amidation of the diester DENDP with 3-amino-1,2-propanediol was performed in MeOH under stirring for 24h.[54] Solid DHPN was collected and triturated with acetone, the precipitate was filtered and recrystallized in MeOH, with a yield of 50%. We have modified this route using Heck reaction C-C coupling palladium catalysed.

Due to its simplicity, we use the Heck reaction here. In our synthesis, the Pd-catalyzed Heck coupling reaction leads to naphthalene and anthracene derivatives **2**, **7, 8** and **10** (Figs. 2 and 3). The Heck reaction mechanism involves a catalytic cycle: (i) oxidative addition of unsaturated halide to a Pd^0 bidentate phosphine ligand giving rise to the Pd^{II} species, (ii) coordination and syn-insertion of the alkene substrate to form the Pd-carbon bond, Pd-R, where R = alkene, (iii) elimination of β or β`-hydride favors the formation of a Pd-alkene complex, and finally (iv) regeneration of the Pd^0 compound by reductive elimination of a halide acid from the base compound, which relies on the presence of a base.[43,44]

As shown in Figs. 2 and 3, in our synthesis scheme dibromo naphthalene **1** and anthracene **6** reacts with ethyl acrylate, sodium vinylsulfonate or carboxyethyl acrylate in the presence of a catalytic amount of palladium-*trans*-di(m-acetate)-bis[di-2-tolylphosphino)benzyl]dipalladium(II) (CataCxiumR®) and $NaOAc{\cdot}3H_2O$ in dimethylformamide (DMF) at 110°C for 10h with stirring, as described by Oliveira et al.[51]; Kessel and Price[52,53] and Nardello et al.[55]. Compounds **2, 8** and **10** were successfully obtained with a yields of 70, 67 and 76%, respectively, of the *trans*-isomer, as previously reported for the Heck coupling reaction.[43,44] However, derivative **7** was not obtained, since crystallization attempts failed and purification by hydrolysis of the compound took place during purification by extraction.

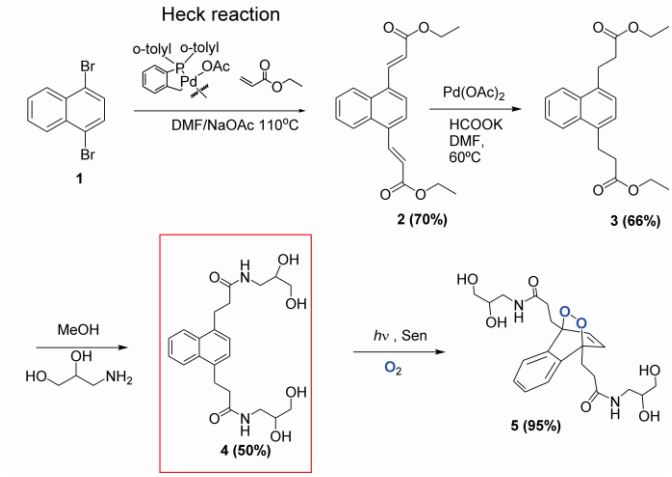

Figure 2- Route of synthesis of the different naphthalene derivatives and their respective endoperoxides.

In the second step of the synthesis, the reduction of the double bond in the α,β-unsaturated ester of derivatives **2** and **10** was achieved by hydrogenation using the Pd-catalyzed reaction in the presence of potassium formate.[56] It has been described that formate salts can easily donate hydrogen and are better than other transfer agents, which could account for the observed release of CO_2 from the hydrogen donor.[56,57] A key step of this strategy is to reduce the double bond in an N_2 atmosphere in the presence of HCOOK as hydrogen donor and $Pd(OAc)_2$ according to Rajagopal and Spatola[57], where $HCOO^-$ is an essential reagent for the reaction to proceed. After successfully applying this method, it was determined that this reaction scheme was less complex and more efficient than the traditional method that utilizes a difficult to control hydrogenation reaction of the aromatic ring using Pd/C with H_2. The Pd-catalyzed reduction of derivatives **2** and **10** yields the desired compounds **3** and **11** with a yield of around 60%. These derivatives were subsequently purified by chromatography.

In the last step of the synthesis, the amidation of the diesters present in derivatives **3, 10** and **11** was performed with 3-amino-1,2-propanediol with stirring for 24h, as in the previous procedure and as described by Martinez et al.[58] This simple procedure generates the corresponding amides**,** in excellent yields. In addition, compounds **4, 13** and **15** were obtained with final product yields of around 50-70%.

After each step, the purity of the compounds was evaluated using ^1H and ^{13}C NMR techniques and each compound was also analyzed by ESI^+ or ESI^- mass spectrometry.

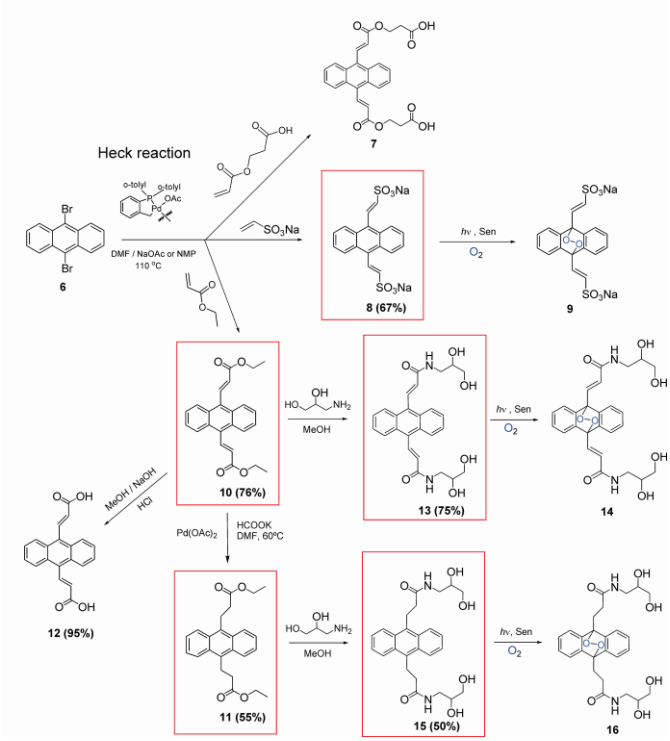

Figure 3: Synthetic steps to reach different anthracene derivatives and their respective endoperoxides.

Spectroscopic Analysis of anthracene derivatives and measure of O_2 ($^1\Delta_g$) quenching.

Anthracene compounds are characterized by three well-resolved absorption bands at around 360 nm and by three defined fluorescence bands at around 400 nm.[59] Fig. 4 shows the absorption and emission spectra of compounds **10** and **15**. For derivative **10** the maximum absorption at 260 and 405 nm and maximum fluorescence emission at 525 nm with excitation at 405 nm in acetonitrile can be observed. Derivative **15** behaves similarly to anthracene with well-defined bands, whereas compound **10** exhibits wide absorption and fluorescence bands, due to the presence of double bonds at the 9,10 position of the anthracene ring producing an electron delocalized structure. All of the compounds synthesized with a double bond (i.e., **2**, 8, **10**, **12** and **13**) present broad absorption and emission bands in the spectra.

It is demonstrated in the literature that anthracene derivatives show higher fluorescence emission and in Table 1 the quantum yield of fluorescence of the anthracene derivatives were obtained and compared to Rhodamine B (at a concentration of 1×10^{-6} molL^{-1} in MeCN; λ_{ex} =400 nm, Φ_{fl} = 0.65)[60] at room temperature. The data show that the fluorescence yield of compound **15** (Φ_{fl}=0.450) is greater than compounds **10** (Φ_{fl} = 0.230)[51] and **11** (Φ_{fl} = 0.352) and closely resembles compound **13** (Φ_{fl} = 0.410), in MeCN/MeOH. As showed by Oliveira et al.[51] the compounds **10** react with O_2 ($^1\Delta_g$) forming the corresponding endoperoxide losing the absorption band at 400 nm and the fluorescence intensity, this demonstrate that anthracene ring is able to react with O_2 ($^1\Delta_g$) by Diels-Alder reaction.

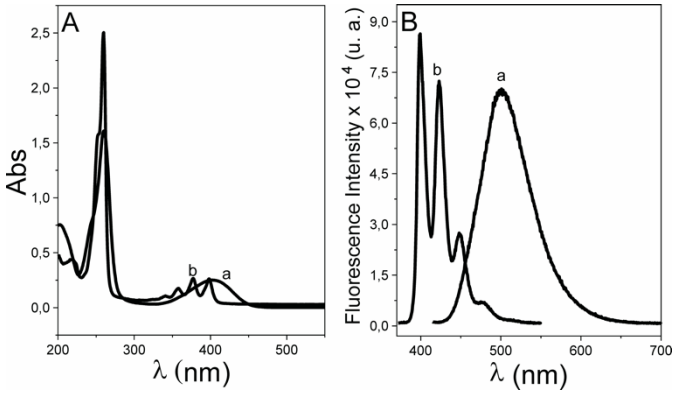

Figure 4: (A) Absorption and (B) emission spectra of compounds (a) **10** and (b) **15** in acetonitrile.

Table 1 presents the total constant quenching (k_t) values of O_2 ($^1\Delta_g$) of the anthracene derivatives. Briefly, the quenching of O_2 ($^1\Delta_g$) produced by an irradiated sample of methylene blue (MB) monitored in MeCN/MeOH (1:1) by recording the monomolecular light emission at 1270 nm in the presence of the anthracene derivatives DMA, DPA, ionic derivative **8** and the synthesized compounds **10**, **11**, **12**, **13** and **15**. 1,3-Diphenylisobenzofuran (DPBF) was used as the standard for O_2 ($^1\Delta_g$) quenching (k_t = 0.66 to 1.04 x 10^9 M^{-1} s^{-1}).[61]

The constants were obtained from the Stern-Volmer graph, by linearly adjusting the experimental plot points of τ_0 / τ versus [Q] denominate K_{sv}, which is equal to the product of the bimolecular quencher constant kq and τ_0. Where, τ_0 and τ are the O_2 ($^1\Delta_g$) lifetime in the absence and presence of the quencher, and [Q] is the quencher concentration.[59] Table 1 present values of k_t and k_r to DPBF as a standard and anthracene derivatives found in the literature and experimental. [51,55]

According to Table 1, the modification in the substituents of the ring is fundamental to the reactivity towards O_2 ($^1\Delta_g$). For example, derivatives **13** and **15** presented higher quenching constants, 1.01 ± 0.01 × 10^7 M^{-1} s^{-1} and 3.75 ± 0.02 × 10^7 M^{-1} s^{-1}, respectively, than derivatives **10** and **11,** 2.20 ± 0.02 × 10^6 M^{-1} s^{-1} and 2.65 ± 0.02 × 10^7 M^{-1} s^{-1}, respectively. It is likely that this difference is attributed to the presence of a diol group attached to a propionic chain through an amide linkage. Moreover, derivative **15** was found to be the most

soluble in water (500 µmolL^{-1}) and derivative **10** was found to be soluble at concentration of 20 µmolL^{-1}.

To derivative **8** experimental data shown a k_t value of 2.7 ± 0.03 × 10^6 M^{-1} s^{-1}, but Nardello et al.[55] reported a value higher of 4.3 x 10^7 M^{-1} s^{-1}. It is interesting to note that Nardelo et al.[55] used the Heck coupling reaction to obtain the water-soluble, ionic anthracene derivative, anthracene-9,10-divinylsulfonate (AVS, **8**, k_t = 4.3 x 10^7 M^{-1} s^{-1}) and showed that the double bonds present in the ring substituents increase the reactivity of the **8**, making it two-times more reactive than derivatives without double bonds, such as anthracene-9,10-diethylsulfonate (AES, k_t = 2.0 x 10^7 M^{-1} s^{-1}).

The reduction of the double bond in **10** could provide insights into the reactivity and structure of these compounds. For example, in this work, the absence of the double bond increased the reactivity of compound **11** nearly ten-fold when compared to derivative **10**, which is in contrast to another study.[55] The presence of the double bond in these derivatives may or may not favor ring activation, and depends on whether the substituent is an electron acceptor or donor. Interestingly, we observed that substituents of anthracenering with donor groups and lacking double bonds had an increased reactivity towards O_2 ($^1\Delta_g$).

Reactivity of naphthalene and anthracene derivatives toward O_2 ($^1\Delta_g$)

Endoperoxide **5** was prepared at low temperature (4°C) using the typical photosensitization method with MB as the photosensitizer, which was removed from the solution using Chelex 100, as reported by Martinez et al.[37] and considering that MB is a photosensitizer generally used by the Type II mechanism, due to its higher singlet oxygen quantum yield (Φ_Δ ~ 0.50),[30,61] obtained a $DHPNO_2$ yield of 95%. The endoperoxide was characterized by HPLC coupled to mass spectrometry and O_2($^1\Delta_g$) generation was evaluated by monomolecular light emission of O_2($^1\Delta_g$) in the near-infrared region.[16]

Mass spectra of the characteristic endoperoxides are depicted in Fig. 5A. Compound **5** presented an intense peak related to the protonated molecule at $[M + H]^+$ = 451 and the presence of an ion at $[M - O_2 - 2H]^+$ = 417, the second peak corresponds to the loss of molecular oxygen and two atoms of hydrogens from **5**, confirming the [4+2] cycloaddition of two atoms of oxygen to the naphthalene ring. The peak of sodium adduct ion is observed at $[M + Na]^+$ = 473.

Additional results showed the characteristic monomolecular emission spectrum of O_2($^1\Delta_g$) in the near-infrared region during the thermodissociation of compound **5** (Fig. 5B), which was also detected with $DMNO_2$, another naphthalene derivative (Fig. 5C). Light emission was monitored, as described previously[16], using a special photon counting apparatus equipped with a monochromator capable of selecting light emission in the near-infrared region (1200–1400 nm). For comparative purposes, the spectra of monomolecular light emission of O_2($^1\Delta_g$) produced by another naphthalene derivative the 1,4-dimethylnaphthalene endoperoxide ($DMNO_2$) was obtained and is presented in Fig. 5C.[20,22]

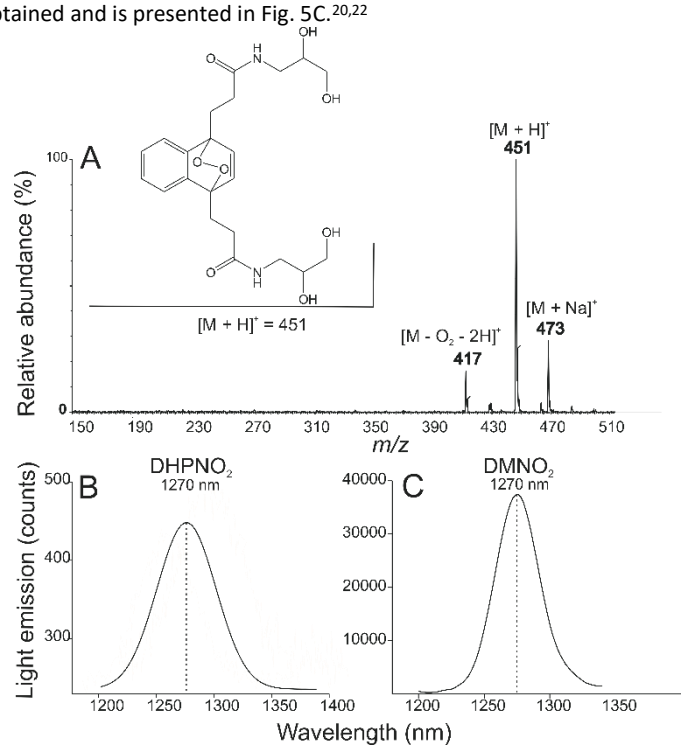

Figure 5. (A) HPLC-MS spectrum of naphthalene derivative **5** endoperoxide and (B) monomol light emission spectra of O_2 ($^1\Delta_g$). Spectrum generated during the thermolysis of the endoperoxides (B) **6** (4 mmolL^{-1} in D_2O) and (C) $DMNO_2$ (10 mmolL^{-1} in methanol) at 37° C.

Table 1. Data obtained for the bimolecular quencher constants (k_t), chemical quencher constants (k_r), the quantum yield of O_2 ($^1\Delta_g$) production and fluorescence for DPBF and anthracene derivatives in acetonitrile/MeOH (1:1).

Quencher	k_t (M^{-1} s^{-1})	k_r (M^{-1} s^{-1})	Φ_Δ	Φ_{fl}
DPBF	1.04 ± 0.11 × $10^{8c,d}$		0.26[a] ± 0.002	----------
	0.66-1.04 × 10^{9b}	----------		
DMA	6.95 ±0.09 × 10^{7d}	21 × $10^{6b,c}$	0.52[a] ± 0.002	0.89[a] ± 0.002
DPA	1.6 ± 0.05 × 10^{6d}	1.2 x $10^{6b,c}$	0.38[a] ± 0.01	0.95[a] ± 0.002
8	2.7 ± 0.03 × 10^{6d}		----------	0.81[e]± 0.003
	4.3 × 10^{7c}	----------		
10	2.20 ± 0.02 × $10^{6c,d}$	1.69± 0.01 × 10^{6c}	0.40 ± 0.1	0.230[c,e] ± 0.002
11	2.65 ± 0.02 × 10^{7d}	--------	-------	0.352[e] ± 0.001
12	1.2 ± 0.01 × 10^{6d}	--------	--------	0.080[e] ± 0.01
13	1.01 ± 0.01 × 10^{7d}	--------	-------	0.410[e] ± 0.002
15	3.75 ± 0.02 × 10^{7d}	--------	--------	0.450[e] ± 0.01

References [a][59,60], [b] [61], [c][51,55]

[d]Values obtained by Stern-Volmer graphics using MB (Φ_Δ ~ 0.50)[62] as a standard of O_2 ($^1\Delta_g$) production.

[e]Rhodamine B and Phenalenone were used as standard for calculating quantum fluorescence yield (Φ_{fl} = 0.65)[60] quantum yield of O_2 ($^1\Delta_g$), respectively.

The generation of O_2 ($^1\Delta_g$) by $DHPNO_2$ **(5)** and $DMNO_2$ was tested using anthracene derivatives. Fig. 6 show the ESI^+ mass spectra for the final component **16,** obtained by trapping O_2 ($^1\Delta_g$) produced by $DHPNO_2$, where the endoperoxide formation with $[M + H]^+$=501 is observed, and an ion with an $[M - O_2 - 2H]^+$ 467 due to the loss of O_2 in the endoperoxide compound.

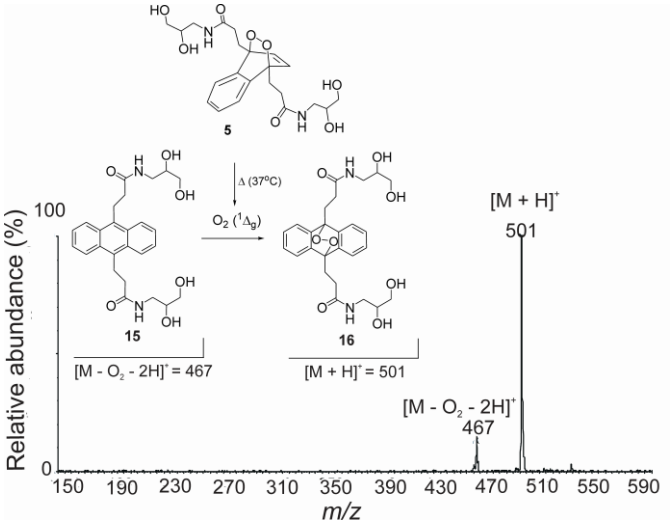

Figure 6. HPLC-MS spectrum of anthracene derivative endoperoxide **16** in the ESI^+ mode.

The HPLC-MS analysis of the products from the reaction between the ionic derivative **8** and O_2 ($^1\Delta_g$), using $DMNO_2$ as a clean source of this species, are shown in Fig. 7. Notably, **8** was almost completely consumed, as evidenced by a single peak corresponding to the endoperoxide $AVSO_2$. This results suggests that the reaction between **8** and O_2 ($^1\Delta_g$) is specific for the formation of the endoperoxide, and does not involve reactions with the vinyl sulfonate groups of the chemical trap.

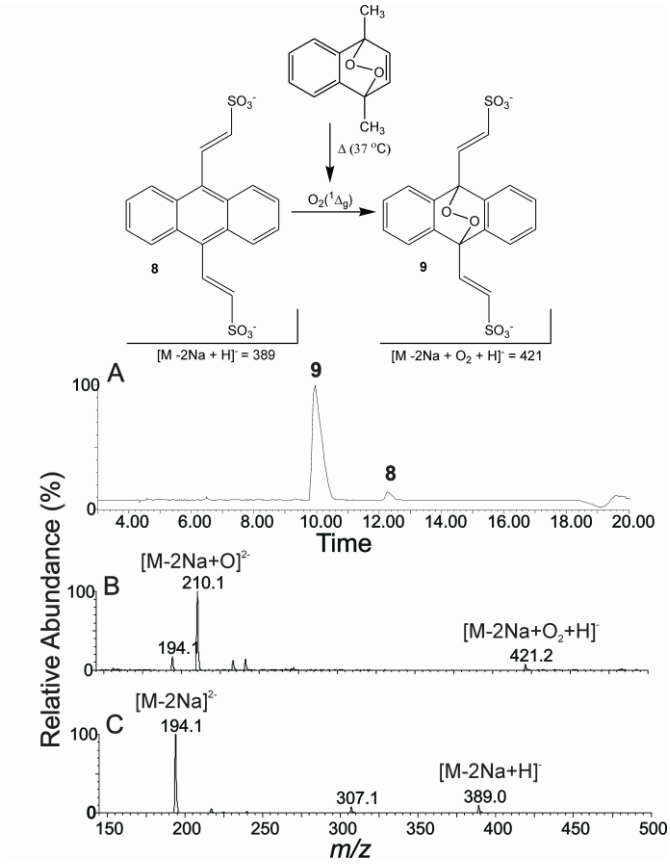

Figure 7. HPLC Chromatogram (A) and MS spectrum of endoperoxide **9** (B) and anthracene derivative **8** (C) in the ESI^- mode.

Since it was proposed that anthracene endoperoxides are the only products of the reaction with O_2 ($^1\Delta_g$) it was decided that it would be interesting to evaluate the reaction of this compound with other reactive oxygen species (ROS) and to also compare it against derivative **10**. The solubilities of compounds **10** and **11** are 0.02 $mmolL^{-1}$ in water, and are increased in acetonitrile/D_2O to 0.1 $mmolL^{-1}$). In Fig. 8 the results of HPLC-MS/MS analysis of the reaction of compound **11** are compared with different ROS. Notably, the correspondent endoperoxide **17**, as show in the Fig. 8 is detected by the MRM method, monitoring a $[M - O_2 - 2H]^+$ 411→377 transition, corresponding to the O_2 ($^1\Delta_g$) produced by $DMNO_2$ and by the $H_2O_2/ClO^-/D_2O$ reaction easily trapped by compound **11**. Small amounts of endoperoxide were also observed in the reaction with $ONOO^-$ and $HO^\bullet$, which may be related to a small quantity of probe used to produce O_2 ($^1\Delta_g$) photochemically in the preparation process.

In the other hand, Myamoto et al.[16] reported that $ONOO^-$ can produce O_2 ($^1\Delta_g$) at neutral to alkaline pH, the production of O_2 ($^1\Delta_g$) was measured using monomol light emission and the anthracene derivative, EAS, as a chemical trap. In the same way, recently Carrier et al.[62] revisited the generation of O_2 ($^1\Delta_g$) during the classical chemical Fenton reaction using the chemical trap, SOSG in the range of pH 4-7. Subsequent HPLC chromatograms (data not shown) indicated that in the presence of HOCl, compound **11** likely reacts with ClO^- and is decomposed. Taken together these results demonstrate that endoperoxide formation is specific for O_2 ($^1\Delta_g$). The same specificity was also observed with compound **10** by Oliveira et al.[51], and shows that the double bond does not interfere with O_2 ($^1\Delta_g$) detection.

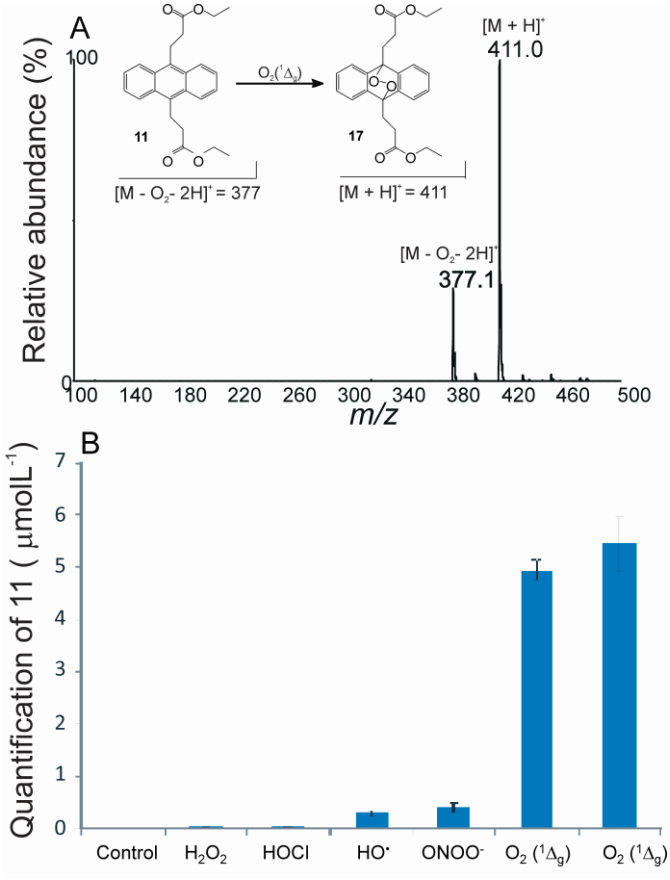

Figure 8: (A) HPLC-MS/MS spectrum of the reaction of compound **11** (0.1 mmolL^{-1} in acetronitrile/D_2O) with O_2 ($^1\Delta_g$). (B) Monitoring corresponding endoperoxide **17** by MRM mode at [M - O_2 - 2H]$^+$ = 411→377 transition in the presence of different ROS. From left to right, reactions with control no ROS, H_2O_2 (1 mmolL^{-1}), ClO^- (1 mmolL^{-1}), $OH^•$, $ONOO^-$ (1 mmolL^{-1}), O_2 ($^1\Delta_g$) reproduced by $DMNO_2$ at 37 °C and O_2 ($^1\Delta_g$) by the reaction of ClO^- with H_2O_2, incubation for 30 min with stirring at 700 rpm in room temperature.

Subcellular localization

In an effort to determine subcellular localization, experiments treating cultures of human neuroblastoma cells (strain SH-SY5Y) with derivative **8** with the sulfonate ion substituents were performed. As shown in Fig. 9, cell viability is practically 100% in the presence of up to 5.6 mmolL^{-1}of compound **8** in the culture medium, even after a 24-hour incubation. The nontoxic nature of **8** makes it a potentially useful O_2 ($^1\Delta_g$) trap for studies in cell culture.

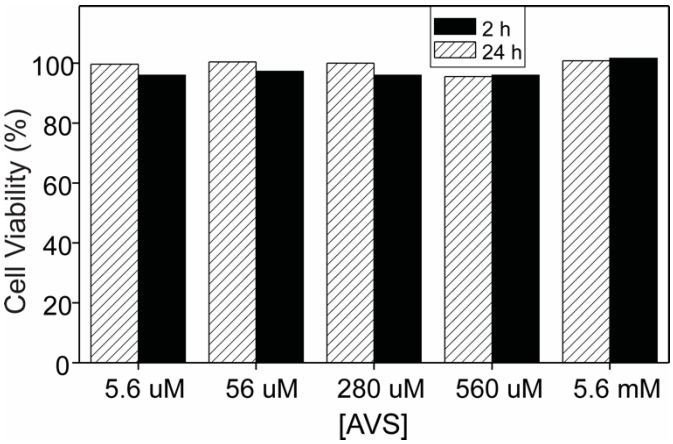

Figure 9. Cell viability of SH-SY5Y human neuroblastoma cells incubated with different concentrations of **8** for 2 or 24 hours.

In order to verify whether or not compound **8** was incorporated into the cells, we employed a fluorescence microscopy approach that allowed us to acquire images, with a green light filter (compound **8,** fluorescence emission), of cells incubated with different concentrations of the compound. Images collected with and without the filter are presented in Fig. 10, and show compound **8** fluorescence is intracellular and not just associated with the membrane.

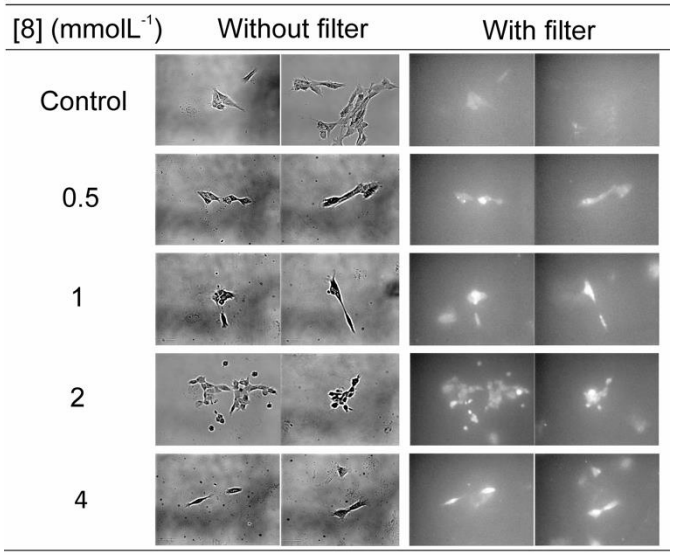

Figure 10. Fluorescence microscopy images of SH-SY5Y human neuroblastoma cells treated with compound **8**. Obtained without and with the green light filter.

Additionally, confocal fluorescence microscopy images for compounds **8**, **10** and **11** are shown in Fig. 11. With regard to **10**, advantages include localization in the membranous compartment and cytoplasm, but not nucleus, which is consistent with observations reported previously by Oliveira et al[51]. Additionally, derivatives **10** and **11** exhibited good cell permeability after 1 and 3h of incubation, but compound **11** had the disadvantage of crystallizing and also agglomerates out of the U87 cells. The lower fluorescence of compound **8**, when compared to the other derivatives is likely due to this derivative being ionic and highly water-soluble. Overall, these results show that even low concentrations of these compounds can

permeate cells and provide further support for the utility of these probes in biological systems.

Moreover, toxicity assays with mammalian fibroblast cells (stain V79) it was found that in the 24h period the probes analyzed did not show effective cytotoxicity as observed for compound **10** derivative in Figure 11D and 11E. The other derivatives **11** and **15** behaved similarly at the same concentrations.

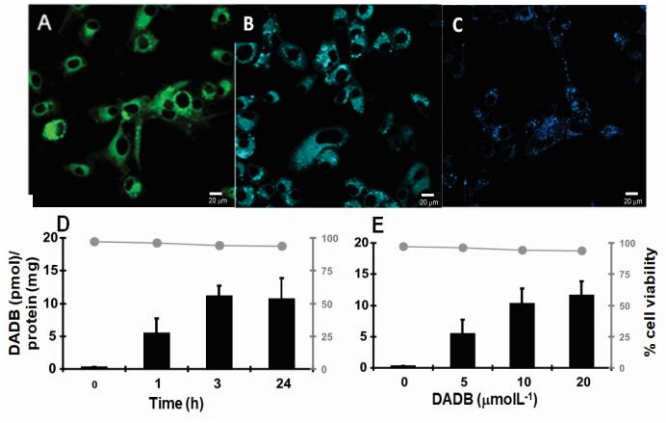

Figure 11. Confocal fluorescence microscopy image of derivatives **10** (A), **11** (B) and **8** (C) (2.5 μmolL^{-1}) in U87 cells after 60 min at incubation. (D) Quantification of **10** at different times and (E) in different concentrations after incubation in V79 cells for 3h. Bars represent the quantification of **10** in cell lysates and the lines represent cell viability assessed by the MTT method.

In our work the results show that a new route of synthesis, with less steps, reagents and time, provides a naphthalene precursor of O_2 ($^1\Delta_g$) generator and several anthracene derivatives that can be used as O_2 ($^1\Delta_g$) traps. The naphthalene endoperoxide **5** has been used for generating O_2 ($^1\Delta_g$) in chemical reactions and also in a few biological systems. The anthracene derivatives are able to cross the lipid membrane and localize inside the cells, as it was found for compounds **8**, **10** and **11.** This constitutes a relevant information for the appropriate utilization of these non-cytotoxic compounds to trap O_2 ($^1\Delta_g$) in biological systems. In addition, studies on derivative 10 involved in photodynamic therapy have already been carried out and showed that this compound can be used to capture O_2 ($^1\Delta_g$) in a cell culture, and we hope that further studies on these derivatives can help to obtain a better probe to be used in biological systems, since derivative **15** presented better solubility in water. This entire study has very interesting information on the use of these compounds to understand the role of O_2 ($^1\Delta_g$) in biological system.

Experimental procedures

Equipment

Absorption and emission spectra of 5 μmolL^{-1} of each derivative were obtained with a model U-3000 spectrophotometer (Hitachi, Tokyo, Japan) and Speg fluorolog spectrophotometer, respectively, using four-sided polished quartz cuvettes with a 1 cm optical path.

Mass spectrometry analysis was performed in a Quattro II mass spectrometer (Micromass, Manchester, UK) with a *Z*-spray atmospheric pressure ionization source in the positive or negative ion mode (ESI^+ or ESI^-). The source and desolvation temperatures were kept at 150ºC and 250ºC, respectively. The optimal flow rates of the drying and nebulizing gases were found to be 300 L h^{-1} and 15 L h^{-1}, respectively. The sample cone and capillary voltage were set to 20 V and 3.5 kV, respectively. The HPLC-MS/MS experiments were recorded on a Shimadzu HPLC system (Tokyo, Japan) equipped with a Phenomenex Gemini C-18 column (250 × 4.6mm i.d, 5 μm particle size). The flow rate of the solution (Solvent A=0.1% formic acid and Solvent B = MeCN or MeOH) was 0.6 mL min^{-1} and a gradient elution of 10 to 100% B over 15 min, 100% B for 5 min, return to 10% B in 5 min, and 10% B for an additional 5 min. The flux directed to the mass spectrometer was set at 0.150 mL min^{-1} and UV detection was set at 220 nm.

^{1}H and ^{13}C NMR spectra were recorded on an Avance DRX 300 spectrometer (Bruker-Biospin, Germany).

To measure O_2($^1\Delta_g$) light emission spectrum, a special photon-counting device developed in our laboratory was used. This piece of equipment consists of a monochromator (800–1400 nm) and a liquid nitrogen-cooled (-80°C) photomultiplier tube (R5509 PMT, Hamamatsu Photoniks KK, Shizuoka, Japan). The applied potential was set to -1.5 kV by a high voltage DC power supply (Model C3360, Hamamatsu Photoniks KK, Shizuoka, Japan). The resulting light emitted in the infrared region from the sample was selected with a monochromator (M300, Bentham Instruments, U.K.) containing a diffraction grating (Type G306R1u0, Bentham Instruments, U.K.). The F900 software was used to control the monochromator and acquire the data. Experiments were conducted in quartz cuvettes and the monomol light emission was monitored during the thermolysis of $DMNO_2$ (10 mmolL^{-1} in methanol) and $DHPNO_2$ (4 mmolL^{-1}, in D_2O).

Synthesis of diethyl N, N'-(1,4-naphthalene)bisacrylate (2)

In a 250 mL three-necked flask, 5 g 1,4-dibromonaphthalene (**1**) (17.5 mmol), 5 g NaOAc·3H_2O (36.8 mmol), and 140 mg of CataCxiumR®(156 mmol) were dissolved in 130 mL of DMF. Then, 5 mL of ethyl acrylate (46.1 mmol) was added, and the reaction was maintained at 110ºC for 16 h with a stirring and cooling system. Next, the solution was cooled to room temperature, residual Pd was removed by filtration and the product was extracted with ether/water. The organic phase was dried, and the residue was recrystallized with MeOH. The employed reaction conditions were in agreement with references Oliveira et al.[51] (yield: 3.3 g, 70%). ^{1}H NMR (300 MHz, $CDCl_3$): δ 1.39 (t, *J* = 7.1 Hz, 3H), 4.34 (q, *J* = 7.1 Hz, 2H), 6.56 (d, *J* = 15.7Hz, 1H), 7.64 (dd, *J* = 6.5 Hz, 3.3 Hz, 2H), 7.76 (s, 1H), 8.24 (dd, *J* = 6.5 Hz, 3.3 Hz, 2H) 8.52 (d, *J* = 15.7Hz, 1H). ^{13}C NMR (300 MHz, $CDCl_3$) δ: 14.59 (CH_3), 60.96 (CH_2), 121.96 (CH), 124.36 (CH), 124.80 (CH), 127.30 (CH), 131.72 (C), 134.16 (C),141.28 (CH), 166.88 (CO). ESI^+-MS *m/z*: 325.

Synthesis of diethyl-1,4-naphthalenedipropanoate (3)

In a 50 mL three-necked flask, 7 mL of DMF was sonicated and bubbled with N_2 for 45 min to completely remove the oxygen dissolved in the solvent. Next, 1.32 g of compound **2** (4.07 mmol) and 66 mg of $Pd(OAc)_2$ (0.29 mmol) were combined and sonicated for 15 min, after which 1.320 g of KCOOH (15.7 mmol) was added. The reaction was maintained in a 60ºC silicone bath in an N_2 atmosphere for 6 h with stirring. The solution was cooled to room temperature and then Et_2O and a saturated $NaHCO_3$ solution were added. The organic layer was separated, washed three times with water and dried with Na_2SO_4. Finally, the solvent was evaporated, and the residue was purified by flash chromatography on silica gel eluted with n-hexane/AcOEt (90:10), according to S. Rajagopal and A. F. Spatola[57] and Arcadi et al.[56] (yield: 0.88 g, 66%.). ^{1}H NMR (300 MHz, $CDCl_3$): δ 1.25 (t, *J* = 7.1 Hz, 3H), 2.74 (t, *J* = 7.3 Hz, 2H), 3.39 (t, *J* = 7.3Hz, 2H), 4.16 (q, *J* = 7.1Hz, 2H), 7.27 (s, 1H), 7.54 (dd, *J* = 6.5, 3.3 Hz, 1H), 8.07 (dd, *J* = 6.5, 3.3 Hz, 1H). ^{13}C NMR (300 MHz, $CDCl_3$) δ:

14.46 (CH_3), 28.38 (CH_2), 35.49 (CH_2), 60.72 (CH_2), 124.49 (CH), 125.88 (CH) 125.97 (CH), 132.21 (C),135.65 (C), 173.27 (CO). ESI^+-MS *m/z*: 329.

Synthesis of N,N'-di(2,3-dihydroxypropyl)-1,4-naphthalenedipropanamide (4).

The amidation reaction was performed by stirring a solution of **3** (80 mg, 0.21 mmol) and 3-amino-1,2-propanediol (0.2 g, 2.2 mmol) in 7 mL MeOH and 4 mL of isopropanol for 24 h. After evaporation of the solvent, 5 mL of acetone was added to the residue. The colorless precipitate was filtered, and recrystallized in MeOH, according Martinez et al.[37,38,58] (yield: 40.5 mg, 50%). ^{1}H NMR (300 MHz, D_2O) *d:* 2.70 (t, J = 7.3 Hz, 3H), 2.84 (dd, J= 13.9, 6.8 Hz, 1H), 2.90 (dd, J=13.9, 5.4 Hz, 1H), 3.01 (dd, J=11.9, 4.1 Hz, 1H), 3.10 (dd, J=11.9, 6.3 Hz, 1H) 3.17 (t, J=7.3 Hz, 2H),3.40 (m, 1H), 7.15 (s, 1H) 7.54 (dd, J=6.5, 3.2 Hz, 2H), 8.05 (dd, J=6.9, 3.2 Hz, 4H). ^{13}C NMR (300 MHz, D_2O): d 28.5 (CH_2), 36.8 (CH_2), 41.9 (CH_2), 63.3 (CH_2), 70.4 (CH), 124.2 (CH), 126.2 (CH), 126.4 (CH) 131.7 (C), 135.2 (C), 176.8 (CO).ESI^+-MS: *m/z* = 451.

Synthesis of N,N'-di(2,3-dihydroxypropyl)-1,4-naphthalenedipropanamide endoperoxide (5)

The $DHPNO_2$ synthesis was carry out according Martinez et al.[37] procedure. The conventional photochemical method of photosensitization with MB was used for the preparation of $DHPNO_2$. In a 50-mL flask, 200 mg of DHPN was dissolved in 2 mL of D_2O under slight heating contained 5 µL of a MB solution (10 mg/mL). The reaction took place in a thermally insulated flask connected to a bath, maintaining the temperature at 4 °C, DHPN was heated gently to be dissolved, in the dark. After that, the solution was stirring and irradiated with a 500 W lamp under a constant oxygen bubble for 5h, with a 30 cm of distance and maintained at 4 °C. Then, Chelex 100 cation-exchange resin was added and the solution was stirred for 20 min at 4 °C until complete MB fixation. Finally, the solution was filtered using a polymeric membrane (0.45 µm) and stored at -80 °C**.**

The anthracenes endoperoxides were synthesized using the same procedure, but the endoperoxides were purified using a solid phase extraction (SPE) cartridge C18 with MeOH, the solution was added in the cartridge and washed three times to remove MB completely. After each addition the cartridge was washed three times.

Synthesis of anthracene-9,10-divinylsulfonate (8)

In a 500 mL flask, 15 g of **6** (DBA - 44.6 mmol), 14.9 g of $NaOAC.3H_2O$ (109.6 mmol), 413.3 mg of trans-di (µ -acetate) -bis [o-(di-o-tolylphosphino) benzyl] dipaladium (II) (CataCXium C® - 459 mmol) and a mixture of N, N-dimethylformamide (DMF - 165 mL) and 1-methyl-2 -pyrrolidone (NMP - 165 mL) were combined and heated to 100°C until a clear solution was obtained. Then, 40 mL of an aqueous sodium vinylsulfonate solution, previously concentrated by evaporation from 56 ml of a 25% aqueous sodium vinylsulfonate solution, was added. The reaction mixture was kept refluxed for 18 h at 110°C), and after cooling the precipitate was recovered by filtration. The insoluble metallic palladium residue was removed from the precipitate by hot filtration from a 325 mL 6/7 water/ethanol reflux mixture according Nardello et al.[55] (yield: 10.05 g, 67%). ^{1}H NMR (300 MHz, acetone-d_6): δ 7.77 (dd, *J* = 6.79, 3.28 Hz, 2H), 7.50 (dd, *J* = 6.85, 3.28 Hz, 2H), 7.30 (d, *J* = 15.78 Hz, 1H), 6.33 (q, *J* = 15.81 Hz, 1H). ^{13}C NMR (300 MHz, Acetone-d_6) δ: 133.25 (CH), 135.99 (CH), 127.69 (C), 128.77 (C), 125.25 (C=C), 126.32 (C=C). ESI^--MS *m/z*: 389.

Synthesis of 3,3 '- (9,10-anthracenediyl) bisacrylate (10)

In a 250 mL three-necked flask, 5 g de compound **6** (17.5 mmol), 5 g $NaOAc{\cdot}3H_2O$ (36.8 mmol), and 140 mg of CataCxiumR®(156 mmol) were dissolved in 130 mL of DMF. Then, 5 mL of ethyl acrylate (46.1 mmol) was added and the reaction was 110 °C for 10 h with a stirring and cooling system. Next, the solution was cooled to room temperature and Pd residues were removed by filtration, as described in Oliveira et al.[51] (yield: 4.24 g, 76%). ^{1}H NMR (300 MHz, acetone-d_6): δ 8.57 (d, *J* = 16.02 Hz, 1H), 8.26 (dd, *J* = 6.80, 3.32 Hz, 2H), 7.61 (dd, *J* = 6.83, 3.30 Hz, 2H), 6.39 (d, *J* = 16.02 Hz, 1H), 4.34 (q, *J* = 7.12 Hz, 2H), 1.36 (t, *J* = 7.12 Hz, 3H). ^{13}C NMR (300 MHz, Acetone-d_6) δ: 15.34 (CH_3), 61.97 (CH_2), 127.24 (CH), 127.90 (CH), 129.66 (CH), 130.32 (C), 132.49 (C), 142.83 (CH), 206.87 (CO). ESI^+-MS *m/z*: 375.

Synthesis of diethyl 9,10-anthracenedipropionate (11)

In a 50 mL three-necked flask, 7 mL of DMF was sonicated and bubbled with N_2 for 45 min. Next, 440 mg of compound **10** (1.18 mmol) and 22 mg of $Pd(OAc)_2$ (0.098 mmol) were added and sonicated for 15 min, after which 440 mg of KCOOH (5.28 mmol) was added. The reaction was maintained in a 60°C silicone bath in an N_2 atmosphere for 6 h. The solution was cooled to room temperature and Et_2O and a saturated $NaHCO_3$ solution were added. The organic layer was separated, washed three times with water, and dried with Na_2SO_4. The solution was then dried and recrystallized with MeOH, according to S. Rajagopal and A. F. Spatola[57] and Arcadi et al.[56] (yield: 0.88 g, 55%). ^{1}H NMR (300 MHz, $CDCl_3$): δ 8.33 (dd, *J* = 6.80, 3.32 Hz, 2H), 7.55 (dd, *J* = 6.83, 3.30 Hz, 2H), 4.22 (q, *J* = 7.12 Hz, 2H), 3.97 (t, J = 7.13 Hz, 2H), 2.79 (t, J = 7.13 Hz, 2H), 1.29 (t, *J* = 7.12 Hz, 3H). ESI^+-MS *m/z*: 377.

Synthesis of N- (2,3-Dihydroxypropyl) -3- {10- [2- (2,3-dihydroxypropylcarbamoyl) -vinyl] -anthracen-9-yl} -acrylamide (13).

In a 25 mL flask, 200 mg of compound **10** (0.53 mmol) was solubilized in a mixture of 17 mL methanol and 10 mL isopropanol, after which 540 mg 3-amino-1,2-propanediol (5.9 mmol) was added. The solution was stirred and refluxed for 36 h. The reaction was monitored with CCD using ethyl acetate as the eluent. At the end of this step, the solvent was removed by rotoevaporation and the product was washed several times with ethyl acetate, centrifuged, and dried according Martinez et al.[37,38,58] (yield: 0.145 g, 75%.). ^{1}H NMR (DMSO-d_6): δ 7.45 (d, *J* = 16.02 Hz, 1H), 7.35 (4H, dd, J = 6.9, 3.2 Hz), 6.77 (4H, dd, J = 6.9, 3.3 Hz), 5.73 (d, *J* = 16.02 Hz, 1H), 3.79 (4H, t, J = 8.3 Hz), 2.80 (2H, m), 2.62 (2H, dd, J = 11.5, 4.9 Hz), 2.55 (2H, dd), 2.35 (2H, dd, J = 13.8, 6.8 Hz), 1.66 (4H, t, J = 8.3 Hz). ^{13}C NMR (300 MHz, DMSO-d_6): δ 25.0 (CH_2), 42.15 (CH_2), 54.50 (CH_2), 63.43 (CH_2), 70.08 (CH), 125.29 (CH),125.80 (CH), 127.98 (C), 130.76 (C), 164.68 (CO). ESI^+-MS *m/z*: 465.

Synthesis of Diethyl 3,3 '- (9,10-anthracenediyl) diacrylic acid (12)

In a 500 mL flask equipped with a reflux condenser, 500 mg of compound **10** (1.34 mmol) was dissolved in 66 mL NaOH and 44 mL MeOH. The system was heated under reflux and stirred for 3 h. Next, concentrated HCl was added to the filtrate until the solution was pH 1 and a precipitate formed. The solution was refrigerated for one night for total precipitation of the compost, and was then filtered and dried (yield: 0.44 g, 95%) ^{1}H NMR (300 MHz, $CDCl_3$): δ 8.57 (d, *J* = 16.02 Hz, 1H), 8.24 (dd, *J* = 6.80, 3.32 Hz, 2H), 7.65 (dd, *J* = 6.83, 3.30 Hz, 2H), 6.34 (d, *J* = 16.02 Hz, 1H). ESI^+-MS *m/z*: 317.

Synthesis of N,N′-di(2,3-dihydroxypropyl)-9,10-anthracenedipropanamide (15).

The amidation reaction was performed by stirring 80 mg of compound **11 (**0.21 mmol) and 0.2 g of 3-amino-1,2-propanediol (2.2 mmol) in 7 mL MeOH and 4 mL of isopropanol for 24 h. After evaporation of the solvent, 5 mL of acetone was added to the residue. The colorless precipitate was filtered, and recrystallized in MeOH, according Martinez et al.[37,38,58] (yield: 40.5 mg, 50%). ^{1}H NMR (DMSO-d_6): δ 7.62 (4H, dd, J = 6.9, 3.2 Hz), 6.75 (4H, dd, J = 6.9, 3.3 Hz), 3.17 (4H, t, J = 8.3 Hz), 2.80 (2H, m), 2.72 (2H, dd, J = 11.5, 4.9 Hz), 2.41 (2H, dd), 2.38 (2H, dd, J = 13.8, 6.8 Hz), 1.86 (4H, t, J = 8.3 Hz). ^{13}C NMR (300 MHz,DMSO-d_6): δ 24.0 (CH_2), 37.2 (CH_2), 42.4 (CH_2), 63.7 (CH_2), 70.7 (CH), 125.0 (CH),125.4 (CH), 129.6 (C), 132.4 (C), 174.6 (CO). ESI$^+$-MS *m/z*: 491.

Reactivity of compound 11 with different ROS

The quantification of endoperoxide of **11** presence in the reactions with different sources of ROS was analyzed by HPLC-MS/MS. A calibration curve with the endoperoxide was obtained at different concentrations of 0.5, 2, 4, 8 and 12 μmolL^{-1} and the samples were quantified by mass spectrometry in the MRM mode. Endoperoxide was synthesized by the photosensitization reaction with MB.

Derivative 1,4-Dimethylnaphthalene endoperoxide ($DMNO_2$) was used as a clean source of O_2 ($^1\Delta_g$) to evaluate the reaction between compound **11** and O_2 ($^1\Delta_g$). In this case, $DMNO_2$ (2 mmolL^{-1} final concentration) was added to 0.1 mmolL^{-1} of compound **11** in acetonitrile/D_2O (1: 1 v/v). The reaction was allowed to proceed for 30 min at 37°C and the sample solutions were analyzed using HPLC-MS/MS.

For reactions with compound **11**, in the presence of H_2O_2 and HOCl, the concentrations of H_2O_2 and HOCl solutions were measured by absorption at 240 nm (ε= 43.6 M^{-1} cm^{-1} in water) and 292 nm (ε = 350 M^{-1} cm $^{-1}$ in 10 mM NaOH), respectively. For $ONOO^-$ the absorption at 302 nm was used to calculate the concentration (ε = 1670 M^{-1}.cm^{-1} in 10 mmolL^{-1} NaOH). The production of $OH^•$ involved the Fenton reaction conducted with H_2O_2, $FeSO_4$ and final dilutions with acetonitrile/phosphate buffer, prepared in 15 mmolL^{-1} D_2O, pH 7.4. All reactions were carried out for 30 min at 37°C with shaking at 750 rpm.

Calculation of total (k_t) and chemical (k_r) quenching rate constants.

Singlet molecular oxygen measurements were carried out in a multifunctional time-resolved fluorimeter with a Hamamatsu R5509 PMT and an Nd:YAG pulsed laser (5 ns) at 532 nm. MB was used as the photosensitizer to obtain the total quenching constant (k_t). Singlet molecular oxygen monomolecular light emission in the near-infrared region was monitored at 1270 nm**.** 1,3-Diphenylisobenzofuran (DPBF) was used as a standard acceptor of O_2($^1\Delta_g$) (literature value, k_t = 1.4 × 10^9 M^{-1} s^{-1}).[60] Stock solutions of DPBF and anthracene derivatives (5 and 10 mmolL^{-1}, respectively) were prepared in MeCN/MeOH and protected from the light. The MB solutions had an optical density of approximately 0.3 at 532 nm. Stern–Volmer quenching experiments were performed by adding aliquots of DPBF or anthracene derivatives (5 to 1000 mL) directly to a cuvette containing MB in MeCN. Quenching concentrations of DPBF and anthracene derivatives ranged from 0 to 160 mmolL^{-1} and 0 to 1000 mmolL^{-1}.

Cell Cultures

The U87 cells (a human primary cell line known as glioblastoma, the most common type of brain cancer) were thawed and transferred to a small bottle and 9 mL of MEM medium was added for a final volume of 10 mL. The cells were grown in MEM medium (pH 7.4) enriched with 10% (v/v) fetal bovine serum (FBS), penicillin (0.04 g/L) and streptomycin sulfate (0.1 g/L). Culture medium without SFB supplementation was sterilized by 0.2 μm filter filtration directly into sterile vials, and sterile SFB was then added. The cells were maintained in a 5% CO_2 atmosphere at 37°C. Cell replication was achieved by washing the cells with sterile PBS (137 mmolL^{-1} NaCl, 2.68 mmolL^{-1} KCl, 1.47 mmolL^{-1} KH_2PO_4, 8 mmolL^{-1} Na_2HPO_4).

Culture of human neuroblastomas

Human neuroblastoma cells (strain SH-SY5Y) were cultured in DEMEM/Nutrient HAM F12 (pH 7.4), enriched with 15% (v / v) FBS, penicillin (0.04 g/L), streptomycin sulfate (0.1 g / L) and $NaHCO_3$ (3.7 g / L). The medium was filtered through a 0.2 μm stop filter to eliminate fungi and bacteria. The cells were incubated in an atmosphere of 5% CO_2/air at 37°C. In the initial stages of cell culturing, a cell suspension was thawed and centrifuged at 1000 rpm for 2 min. Without sterile laminar flow, the supernatant was discarded and the pellet was resuspended in 1 ml of the appropriate medium. After another centrifugation step, the supernatant was discarded again and the pellet was suspended in 1 mL of medium. The resuspended cells were then transferred to a small culture bottle and an additional 9 mL of medium for use. For cell drawing, the medium was aspirated and the cells were washed twice with autoclaved PBS (137 mmolL^{-1} NaCl; 2.68 mmolL^{-1} KCl; 1.47 mmolL^{-1} KH_2PO_4; 8 mmolL^{-1} Na_2HPO_4). Cells were detached with 1.5 ml of 0.05% (w/v) trypsin and after 2 min, 25 mL of medium was added and the entire suspension was transferred to a large bottle. For cell freezing, 1 ml of dimethyl sulfoxide (DMSO) was added to 10 ml of medium in this step and the cell suspension was divided into 10 vials. The bottles were stored in the freezer for 30 minutes, maintained at -80°C for 24 hours and stored in liquid nitrogen.

Cell Quantification

The cells were grown in culture medium with serum (small plate - 3mL of culture medium), in an atmosphere of 5% CO_2 /air at 37 °C. After reaching a confluence of approximately 80%, the medium was removed, the cells were washed with PBS and incubated for 1, 3 and 6 hours in DMEM medium with 10% SBF and different concentrations of DADB (0, 5, 10 and 20 μmolL^{-1}). After the incubation period, cells were washed with PBS, then scraped from the plate with an additional 1 ml of PBS and transferred to a microtube. The samples were frozen and thawed for cell disruption, then 1 mL of $CHCl_3$/MeOH (2: 1) was added to the cell pellet. The organic phase was collected and dried. For the measurement of DADB incorporated into the cells 1000 μL of MeOH was add to the samples before transferring them to a fluorescence cuvette. Initially, a calibration curve was constructed using the DADB standard, using λ_{ex} = 405 nm e λ_{em} = 520 nm.

Cell Viability

The hamster fibroblast-derived V79 strain was grown in DMEM medium (pH 7.4) enriched with 10% (v/v) FBS, penicillin (0.04 g /L), streptomycin sulfate (0 0.1 g /L) and $NaHCO_3$ (3.7g / L). The medium was filtered through a 0.2 μm filter to eliminate fungi and bacteria. Cells were incubated in a 5% CO_2 /air atmosphere at 37°C. For cell replication, the medium was aspirated, and the cells were washed

twice with sterile PBS (137 mmolL^{-1} NaCl; 2.68 mmolL^{-1} KCl; 1.47 mmolL^{-1} KH_2PO_4; 8 mmolL^{-1} Na_2HPO_4).

Approximately 10^4 cells were seeded in 96-well plates with 100 µL culture medium containing 10% FBS and incubated for 24h in a 5% CO_2 atmosphere at 37°C. Prior to compound exposure, the medium was removed, and the cells were washed with PBS. After the exposure period, the medium was aspirated and the cells were incubated for 2 h in 150 µL of serum-free medium with 300 µL of a solution 5 mg/ml of 3- (4,5-dimethyl-2-thiazolyl) -2-bromide, 5-diphenyl-2H-tetrazolium (MTT) in PBS. The supernatant was carefully removed so as to not aspirate the precipitated formazan, which was later resuspended in 200 µl DMSO. The viability of the cells was determined by the absorbance ratios at 570 nm obtained from treated cells and control cells.

Fluorescence microscopy of cells

Cells were cultured on an appropriate microscope slide, immersed in culture medium with serum, in an atmosphere of 5% CO_2/air at 37°C. After reaching a confluence of approximately 80%, the medium was removed, the cells were washed with PBS and incubated in a colorless medium without SFB with different concentrations of compound **8** (0.5, 1, 2 and 4 mmolL^{-1}) for 24 h. After the treatment, the culture medium was removed from the slides, the cells were washed with PBS and visualized under a Diaphot 300 fluorescence optical microscope (Nikon, Tokyo, Japan), using a Xenon lamp and green light filter.

Confocal analysis

Cells (U87) were plated at a density of 2×10^5 on slides placed into 6-well plates. Stock solutions of compounds, **8**, **10** and **11** were prepared in DMSO and diluted in MEM culture medium to a final concentration of 2.5 µmolL^{-1}. Solutions of compounds **8**, **10** and **11** were added to a final volume of 2 mL and incubated for 1h in 5% CO_2 at 37°C. Next, the cells were washed with PBS and 2 mL of 4% formaldehyde was added to fix the cells and the slides were mounted with PBS-glycerol (1:1) and analyzed by confocal microscopy, using a 60× objective. The fluorescence excitation and emission values for each compound are as follows: **8**: λ_{ex} = 355 nm and λ_{em} = 500 nm, **10**: λ_{ex} = 400 nm and λ_{em} = 525 nm and **11**: λ_{ex} = 355 nm and λ_{em} = 500 nm.

Conclusions

We have used an efficient and easily-performed synthesis route to one naphthalene and six anthracene derivatives. In addition to reducing the number of synthetic steps, other advantages of this approach include the simple reaction conditions and relative high percent yields. In future work, naphthalene endoperoxide **5** will be used as the clean $O_2(^1\Delta_g)$ source in these cell experiments with **8**, **10**, **11**, **13**, and **15** traps to quantitate cell killing by $O_2(^1\Delta_g)$ as a function of non-ionic and ionic substituents, where the former would likely reside favorably in membranes. The formation of endoperoxides is of particular interest since these compounds could function as not only a clean chemical source but also traps of $O_2(^1\Delta_g)$ in biological systems. The involvement of $O_2(^1\Delta_g)$ in biological systems has been a topic of interest in a number of studies, and the development of a clean $O_2(^1\Delta_g)$ generating compounds will contribute to a better understanding the role of O_2 ($^1\Delta_g$) in biological system . We have also isolated and identified anthracene derivatives with different substituents at the 9,10 positions and will pursue their utility in future studies.

Conflicts of interest

There are no conflicts to declare.

Acknowledgements

We thank FAPESP (Fundação de Amparo à Pesquisa do Estado de São Paulo) - Paolo Di Mascio n° 2012/12663-1, CEPID Redoxoma – P.D.M., M.H.G.M. n° 2013/07937-8, CNPq (Conselho Nacional de Desenvolvimento Científico e Tecnológico) – P.D.M. n° 302120/2018-1, M.H.G.M. n° 301404/2016-0, CAPES (Coordenação de Aperfeiçoamento de Pessoal de Nível Superior), PRPUSP (Pro-Reitoria de Pesquisa da Universidade de São Paulo) - NAP Redoxoma – P.D.M., M.H.G.M. n° 2011.1.9352.1.8) and John Simon Guggenheim Memorial Foundation (P.D.M. Fellowship) for financial support. M.S.O. and G.C. are fellows from PNPD/CAPES (UEG/CAPES n° 817164/2015, Universal CNPq n° 448297/2014-0, IF Goiano Campus Rio Verde/CAPES n° 88887.342460/2019-00) and CNPq, respectively. A.G. acknowledges funding from the National Science Foundation (CHE-1856765).

Notes and references

1. P. Di Mascio, G. R. Martinez, S. Miyamoto, G. E. Ronsein, M. H. G. Medeiros and J. Cadet, Singlet molecular oxygen reactions with nucleic acids, lipids, and proteins, *Chem. Rev.,* 2019, **119**, 2043-2086.

2. O. Chiarelli-Neto, A. S. Ferreira, W. K. Martins, C. Pavani, D. Severino, F. Faia o-Flores, S. S. Maria-Engler, E. Aliprandini, G. R. Martinez, P. Di Mascio, M. H. G. Medeiros, M. S. Baptista, Melanin photosensitization and the effect of visible light on epithelial cells, *PLOS ONE,* 2014, **9**, 11, e113266.

3. M. J. Beltrán-García, F. M. Prado, M. S. Oliveira, D. Ortiz-Mendoza, A. C. Scalfo, A. Pessoa Jr., M. H. G. Medeiros, J. F. White, P. Di Mascio, Singlet molecular oxygen generation by light-activated DHN-melanin of the fungal pathogen *Mycosphaerella fijiensis* in black Sigatoka disease of bananas, *PLOS ONE*, 2014, **9**, 3, e91616.

4. J.-L. Ravanat, G. R. Martinez, M. H. G. Medeiros, P. Di Mascio and J. Cadet, Mechanistic aspects of the oxidation of DNA constituents mediated by singlet molecular oxygen, *Arch. Biochem. Biophys.,* 2004, **423**, 23–30.

5. G. E. Ronsein, F. M. Prado, F. V. Mansano, M. C. B. Oliveira, M. H. G. Medeiros, S. Miyamoto and P. Di Mascio, Detection and characterization of cholesterol-oxidized products using HPLC coupled to dopant assisted atmospheric pressure photoionization tandem mass spectrometry, *Anal. Chem.,* 2010, **82**, 7293-7301.

6. F. V. Mansano, R. M. A. Kazaoka, G. E. Ronsein, F. M. Prado, T. C. Genaro-Mattos, M. Uemi, P. Di Mascio and S. Miyamoto, Highly sensitive fluorescent method for the detection of cholesterol aldehydes formed by ozone and singlet molecular oxygen, *Anal. Chem.,* 2010, **82**, 6675-6781.

7. V. Duarte, D. Gasparutto, L. F. Yamaguchi, J.-L. Ravanat, G. R. Martinez, M. H. G. Medeiros, P. Di Mascio and J. Cadet, Oxaluric acid as the major product of singlet oxygen-mediated oxidation of 8-Oxo-7,8-dihydroguanine in DNA, *J. Am. Chem. Soc.,* 2000, **122**, 12622−12628.

8. E. L. Clennan and A. Pace, Advances in singlet oxygen chemistry, *Tetrahedron*, 2005, **61**, 6665−6691.

9. J. M. Aubry and B. Cazin, Chemical sources of singlet oxygen. quantitative generation of singlet oxygen from hydrogen-peroxide disproportionation catalyzed by molybdate Ions, *Inorg. Chem.,* 1988, **27**, 2013−2014.

10. A. E. Cahill and H. Taube, The use of heavy oxygen in the study of reactions of hydrogen peroxide, *J. Am. Chem. Soc.* 1952, **74**, 2312−2318.
11. H. Sies, Oxidative stress: oxidants and antioxidants; Academic Press: London, 1991.
12. H. Sies, Oxidative stress: eustress and distress; Academic Press: London, 2020.
13. J. Cadet and P. Di Mascio, Peroxides in biological systems. In Patai's chemistry of functional groups; John Wiley & Sons, Ltd: Chichester, 2006.
14. C. M. Mano, F. M. Prado, J. Massari, G. E. Ronsein, G. R. Martinez, S. Miyamoto, J. Cadet, H. Sies, M. H. G. Medeiros, E. J. H. Bechara and P. Di Mascio, Excited singlet molecular O_2 ($^1\Delta_g$) is generated enzymatically from excited carbonyls in the dark, *Sci. Reports,* 2014, **4**:5938.
15. C. P. Stanley, G. J. Maghzal, A. Ayer, J. Talib, A. M. Giltrap, S. Shengule, K. Wolhuter, Y. T. Wang, P. Chadha, C. Suarna, O. Prysyazhna, J. Scotcher, L. L. Dunn, F. M. Prado, N. Nguyen, J. O. Odiba, J. B. Baell, J. P. Stasch, Y. Yamamoto, P. Di Mascio, P. Eaton, R. J. Payne and R. Stocker, Singlet molecular oxygen regulates vascular tone and blood pressure in inflammation, *Nature*, 2019, **566**, 548-552.
16. S. Miyamoto, G. E. Ronsein, T. C. Correa, G. R. Martinez, M. H. G. Medeiros and P. Di Mascio, Direct evidence of singlet molecular oxygen generation from peroxynitrate, a decomposition product of peroxynitrite, *Dalton Trans.,* 2009, **29**, 5720–5729.
17. S. Miyamoto, G. R. Martinez, M. H. G. Medeiros and P. Di Mascio, Singlet molecular oxygen generated by biological hydroperoxides, *J. Photochem. Photobiol. B.,* 2014, **139**, 24-33.
18. F. M. Prado, M. C. B. Oliveira, S. Miyamoto, G. R. Martinez, M. H. G. Medeiros, G. E. Ronsein and P. Di Mascio, Thymine hydroperoxide as a potential source of singlet molecular oxygen in DNA, *Free Radical Biol. Med.*, 2009, **47**, 401-409.
19. S. Miyamoto, G. R. Martinez, M. H. G. Medeiros and P. Di Mascio, Singlet molecular oxygen generated from lipid hydroperoxides by the Russell mechanism: studies using ^{18}O-labeled linoleic acid hydroperoxide and monomol light emission measurements, *J. Am. Chem. Soc.,* 2003, **125**, 6172-6179.
20. S. Miyamoto, G. R. Martinez, A. P. Martins, M. H. G. Medeiros and P. Di Mascio, Direct evidence of singlet molecular oxygen [O_2($^1\Delta_g$)] production in the reaction of linoleic acid hydroperoxide with peroxynitrite, *J. Am. Chem. Soc.* 2003, **125**, 4510-4517.
21. S. Miyamoto, G. R. Martinez, D. Rettori, O. Augusto, M. H. G. Medeiros and P. Di Mascio, Linoleic acid hydroperoxide reacts with hypochlorous acid, generating peroxyl radical intermediates and singlet molecular oxygen, *Proc. Natl. Acad. Sci. U.S.A.,* 2006, **103**, 293-298.
22. M. Uemi, G. E. Ronsein, F. M. Prado, F. D. Motta, S. Miyamoto, M. H. G. Medeiros and P. Di Mascio, Cholesterol hydroperoxides generate singlet molecular oxygen [O_2 ($^1\Delta_g$)]: near-IR emission, ^{18}O-labeled hydroperoxides and mass spectrometry, *Chem. Res. Toxicol.* 2011, **24**, 887-895.
23. G. E. Ronsein, M. C. B Oliveira, S. Miyamoto, M. H. G. Medeiros and P. Di Mascio, Tryptophan oxidation by singlet molecular oxygen [O_2 ($^1\Delta_g$)]: Mechanistic studies using O-18-labeled hydroperoxides, mass spectrometry, and light emission measurements, *Chem. Res. Toxicol.* 2008, **21**, 1271-1283.
24. G. E. Ronsein, M. C. B Oliveira, M. H. G. Medeiros and P. Di Mascio, Characterization of [O_2 ($^1\Delta_g$)]-derived oxidation products of tryptophan: A combination of tandem mass spectrometry analyses and isotopic labeling studies, *J. Am. Soc. Mass Spectrom.,* 2009, **20**, 188 –197.
25. P. Di Mascio, A. R. Sundquist, T. P. A. Devasagayam and H. Sies, Assay of lycopene and other carotenoids as singlet oxygen quenchers, *Methods Enzymol*., 1992, **213**, 429-438.
26. A. P. Castano, T. N. Demidova and M. R. Hamblin, Mechanisms in photodynamic therapy: Part one-photosensitizers, photochemistry and cellular localization., *Photodiagn. Photodyn. Ther*., 2004, **1**, 279−293.
27. R. M. Tyrrell, Role for Singlet Oxygen in Biological Effects of Ultraviolet A Radiation, *Methods Enzymol.,* 2000**, 319**, 290−296.
28. C. S. Foote, Mechanisms of photosensitized oxidation. There are several different types of photosensitized oxidation which may be important in biological systems, *Science*, 1968, **162**, 963−970.
29. C. S. Foote, Definition of type I and type II photosensitized oxidation., *Photochem. Photobiol*., 1991, **54**, 659.
30. M. S. Baptista, J. Cadet, P. Di Mascio, A. A. Ghogare, A. Greer, M. R. Hamblin, C. Lorente, S. C. Nunez, M. S. Ribeiro, A. H. Thomas, M. Vignoni, T. M. Yoshimura, Type I and type II photosensitized oxidation reactions: Guidelines and mechanistic pathways, *Photochem. Photobiol*., 2017, **93**, 912−919.
31. H. H. Wasserman, K. B. Wiberg, D. L. Larsen,, J. Parr, Photooxidation of methylnaphthalenes, *J. Org. Chem*., 2005, **70**, 105-109.
32. H. H. Wasserman and D. L. Larsen, Formation of 1,4-endoperoxide from the dye-sensitized photooxygenation of alkyl naphthalenes, *J. Chem. Soc., Chem. Commun*., 1972, **5**, 253-4.
33. C. Pierlot, J.-M. Aubry, K. Briviba, H. Sies and P. Di Mascio, Naphthalene endoperoxides as generators of singlet oxygen in biological media. *Methods Enzymol*. 2000, **319**, 3−20.
34. C. Pierlot, S. Hajjam, C. Barthelemy and J.-M. Aubry, Water-soluble naphthalene derivatives as singlet oxygen ($^1O_2$, $^1\Delta_g$) carriers for biological media, *J. Photochem. Photobiol., B.* 1996, **36**, 31–39.
35. A. Dewilde, C. Pellieux, C. Pierlot, P. Wattre, and J.-M. Aubry, Inactivation of intracellular and 3,3'-(1,4-Naphthylidene)dipropionate. Monomol and dimol photoemission and the effects of 1,4-diazabicyclo[2.2.2]octane, *Biol. Chem.,* 1998, **379**, 1377.
36. L.-O. Klotz, C. Pellieux, K. Briviba, C. Pierlot, J-M. Aubry and H. Sies, Mitogen-activated protein kinase (p38-, JNK-, ERK-) activation pattern induced by extracellular and intracellular singlet oxygen and UVA*, Eur. J. Biochem. FEBS,* 1999, **260**, 917-922.
37. G. R. Martinez, J. -L. Ravanat, M. H. G. Medeiros, J. Cadet and P. Di Mascio, Synthesis of a naphthalene endoperoxide as a source of ^{18}O-labeled singlet oxygen for mechanistic studies, *J. Am. Chem. Soc.,* 2000**, 122**, 10212–10213.
38. G. R. Martinez, M. H. G. Medeiros, J-L. Ravanat, J. Cadet and P. Di Mascio, Naphthalene endoperoxide as a source of [^{18}O]-labeled singlet oxygen for oxidative DNA damage studies, *Trends Photochem. Photobiol.,* 2002, **9**, 25–39.
39. P. Di Mascio and H. Sies, Quantification of singlet oxygen generated by thermolysis of 3,3'-(1,4-naphthylidene)dipropionate. Monomol and dimol photoemission and the effects of 1,4-diazabicyclo[2.2.2]octane, *J. Am. Chem. Soc.,* 1989, **111**, 2909-2914
40. C. Pellieux, A. Dewilde, C. Pierlot and J.-M. Aubry, Bactericidal and virucidal activities of singlet oxygen generated by thermolysis of naphthalene endoperoxides, *Methods Enzymol*., 2000, **319**, 197-207.
41. J.-M. Aubry, In *Membrane Lipid Oxidation;* Vigo-Pelfrey, C., Ed., CRC Press, Boca Raton, 1991, 2.
42. P. Di Mascio, E. J. H. Bechara and J.C. Rubim, Dioxygen NIR FT-Emission ($^1\Delta_g \rightarrow {}^1\Sigma_g$) and Raman spectra of 1,4-dimethylnaphthalene endoperoxide: a source of singlet molecular oxygen. *Appl. Spectrosc.,*1992, **46**, 236-239.

43. M. Shibasaki, E. M. Vogl and T. Ohshima, Asymmetric Heck reaction, *Adv. Synth. Catal.,* 2004, **346**, 1533-1552.
44. R. F. Heck and J. P. Nolley, Palladium-Catalyzed vinylic hydrogen substitution reactions with aryl, benzyl, and styryl halides, *J. Org. Chem.*, 1972, **14**, 2320-2322.
45. W. Fudickar and T. Linker, Why triple bonds protect acenes from oxidation and decomposition, *J. Am. Chem. Soc.* 2012, **134**, 15071-15082.
46. W. Fudickar and T. Linker, Synthesis of pyridylanthracenes and their reversible reaction with singlet oxygen to endoperoxides, *J. Org. Chem.* 2017, **82**, 17, 9258-9262
47. W. Fudickar and T. Linker, Release of singlet oxygen from aromatic endoperoxides by chemical triggers, *Angew. Chem.*, 2018, **57**, **39**, 12971-12975.
48. C. Flors, M. J. Fryer, J. Waring, B. Reeder, U. Bechtold, P. M. Mullineaux, S. Nonell, M. T. Wilson and N. R. Baker, Imaging the production of singlet oxygen in vivo using a new fluorescent sensor, Singlet Oxygen Sensor Green, *J. Exp. Bot.*, 2006, **57**, 1725–1734.
49. N. Umezawa, K. Tanaka, Y. Urano, K. Kikuchi, T. Higuchi and T. Nagano, Novel fluorescent probes for singlet oxygen, *Angew. Chem. Int. Ed.,* 1999, **38**, 19.
50. K. Tanaka, T. Miura, N. Umezawa, Y. Urano, K. Kikuchi, T. Higuchi and T. Nagano, Rational design of fluorescein-based fluorescence probes. Mechanism-based design of a maximum fluorescence probe for singlet oxygen, *J. Am. Chem. Soc.*, 2001, **123**, 2530–2536.
51. M. S. Oliveira, D. Severino, F. M. Prado, J. P. F. Angeli, F. D. Motta, M. S. Baptista, M. H. G. Medeiros and P. Di Mascio, Singlet molecular oxygen trapping by the fluorescent probe diethyl-3,3'-(9,10-anthracenediyl)bisacrylate synthesized by the Heck reaction, *Photochem. Photobiol. Sci.,* 2011, **10**, 1546−1555.
52. D. Kessel and M. Price, Evaluation of diethyl-3-3'-(9,10-anthracenediyl)*bis* acrylate as a probe for singlet oxygen formation during photodynamic therapy, *Photochem. Photobiol*., 2012, **88**, 717–720.
53. M. Price and D. Kessel, On the use of fluorescence probes for detecting reactive oxygen and nitrogen species associated with photodynamic therapy, *J Biomed Opt.*, 2010, **15**, 5, 051605.
54. A. I. Vogel, In *Vogel's Textbook of Practical Organic Chemistry*; revised by Furniss, B.S., Hannaford, A. J., Smith, P. W. G., Tatchell, A. R., John Wiley & Sons: New York, 1989.
55. Nardello, V.; Aubry, J. M.; Johnston, P.; Bulduk, I.; Vries, A. H. M.; Alsters, P. L. Facile preparation of the water-soluble singlet oxygen traps anthracene-9,10-divinylsulfonate (AVS) and anthracene-9,10-diethylsulfonate (AES) via a heck reaction with vinylsulfonate. *Synlett*. 2005, **17**, 2667–2669.
56. A. Arcadi, E. Bernocchi, S. Cacchi, F. Marinelli, Palladium-Catalyzed conjugate reduction of α,β-unsaturated carbonyl compounds with potassium formate, *Synlett*, 1991, **01**, 27-28.
57. S. Rajagopal and A. F. Spatola, Mechanism of palladium-catalyzed transfer hydrogenolysis of aryl chlorides by formate salts. *J. Org. Chem.*, 1995, **60**, 1347-1355.
58. G. R. Martinez, F. Garcia, L. H. Catalani, J. Cadet, M. C. B. Oliveira, G. E. Ronsein, S. Miyamoto, M. H. G. Medeiros and P. Di Mascio, Synthesis of a hydrophilic and non-ionic anthracene derivative, the *N,N'*-di-(2,3-dihydroxypropyl)-9,10-anthracenedipropanamide as a chemical trap for singlet molecular oxygen detection in biological systems, *Tetrahedron*, 2006, **62**, 10762−10770.
59. J. R. Lakowicz, *Principles of Fluorescence Spectroscopy*, 3ed, Springer, *Baltimore, Maryland, USA,* pp. 8-12.
60. M. Montalti, A. Credi, L. Prodi and M. T. Gandolfi, *Handbook of Photochemistry*, Third edition, Taylor & Francis Group, 2006, pp. 574.
61. F. Wilkinson, W. P. Helman and A. B. Ross, Rates constants for the decay and reactions of the lowest electronically excited singlet state of molecular oxygen in solutions. An expanded and revised compilation, *J. Phys. Chem. Ref. Data,* 1995, **24**, 779.
62. A. J. Carrier, S. Hamid, D. Oakley, K. Oakes and X. Zhanga, Singlet oxygen generation in classical fenton chemistry, preprint, ChemRxiv, 2019.

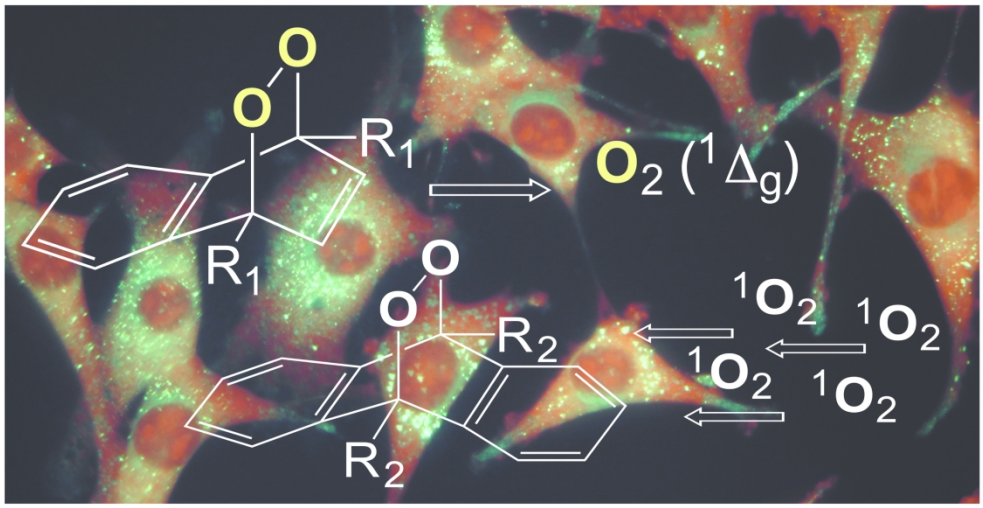

"Facile thermal release of O_2 ($^1\Delta_g$) [$^1O_2$] by naphthalene endoperoxide, and subsequent $^1O_2$ capture by anthracene traps to form stable anthracene endoperoxides. This enables an exploration of $^1O_2$ formation and capture within cells."

285x160mm (300 x 300 DPI)